applied sciences

MDPI

Article

3D Printed Robotic Hand with Piezoresistive Touch Capability

Gonçalo Fonseca [1,2], João Nunes-Pereira [1,*] and Abílio P. Silva [1,*]

[1] Centre for Mechanical and Aerospace Science and Technologies (C-MAST), Universidade da Beira Interior, Rua Marquês d'Ávila e Bolama, 6201-001 Covilhã, Portugal
[2] BEDEV Lda, Bioengeneering Development, Ubimedical, 6200-284 Covilhã, Portugal
* Correspondence: j.nunespereira@ubi.pt (J.N.-P.); abilio@ubi.pt (A.P.S.)

Abstract: This work proposes the design of a low-cost sensory glove system that complements the operation of a 3D-printed mechanical hand prosthesis, providing it with the ability to detect touch, locate it and even measure the intensity of associated forces. Firstly, the production of the prosthetic model was performed using 3D printing, which allowed for quick and cheap production of a robotic hand with the implementation of a mechanical system that allows controlled movements with high performance and with the possibility of easily replacing each piece individually. Secondly, we performed the construction and instrumentation of a complementary sensory mimicry add-on system, focusing on the ability to sense touch as the primary target. Using piezoresistive sensors attached to the palm of the glove, a multi-sensor system was developed that was able to locate and quantify forces exerted on the glove. This system showed promising results and could be used as a springboard to develop a more complex and multifunctional system in the future.

Keywords: 3D printing; prosthetic hand; sensory system; piezoresistive sensors

Citation: Fonseca, G.; Nunes-Pereira, J.; Silva, A.P. 3D Printed Robotic Hand with Piezoresistive Touch Capability. *Appl. Sci.* **2023**, *13*, 8002. https://doi.org/10.3390/app13148002

Academic Editor: Laura Cercenelli

Received: 7 June 2023
Revised: 26 June 2023
Accepted: 5 July 2023
Published: 8 July 2023

1. Introduction

The development of prosthetic systems that not only prioritize superior mechanical functionality, such as more complete movement of the mechanical hand with a wider range of finger movement and a greater degree of freedom, but also focus on the sensory aspect is still very limited and in dire need of further research. Focusing on the above aspects, this work proposes the design of a low-cost sensory glove system that complements the functionality of a 3D-printed mechanical robotic hand [1–3].

The choice of 3D printing as a method for manufacturing prostheses allowed for a more controlled production process with cost reduction, maintaining the quality of each individual part and allowing for a wider range of choices in terms of the types of raw materials used [4–7]. The raw materials were selected according to the requirements of parts and the type of function the parts would perform, for example, since the robotic hand has a greater need for resistance regarding mechanical strength than the forearm, these two structures were made with different polymers. Polylactic acid (PLA) was the main material used for the hand parts due to its superior mechanical properties after printing: a tensile yield strength of ≈51 MPa, a tensile modulus of ≈2.3 GPa, a flexural strength of ≈83 MPa and a flexural modulus of ≈3.1 GPa [8]. As the forearm is in direct contact with the user's body and is not subject to the same mechanical stress as the hand, polyethylene terephthalate (PETG) was chosen for its manufacture, as it is biocompatible and can also withstand some mechanical stress: ≈47 MPa tensile yield strength, ≈1.5 GPa tensile modulus and 5.1% elongation at yield point [9].

For the sensory glove system, it was decided to separate the prosthetic and sensory systems, as many patients who tried sensory prototypes could not fully adapt to them. Furthermore, only one type of somatosensory sensation (touch) was studied and/or produced, as the addition of other parameters, such as temperature and proprioception, would result in greater complexity without adequately addressing each parameter individually. As

an example of a multi-layered system, A. Polishchuk et al. [10] developed a multi-sensory glove where, in addition to temperature and humidity, touch measurements using piezoresistive sensors were considered to deepen the information about objects held by the sensory system. The data produced by this system were more complete because it simultaneously reduced the sensing area and evenly distributed the sensors, focusing on very small areas of the palm rather than the main touch areas, and also placed the temperature and humidity sensors in more central areas of the palm of the prosthetic hand, excluding the fingers.

While the use of sensors offers a wider range of applications in health monitoring and human–machine interaction, it also has some drawbacks. The type of mounting has a major impact on quality and aesthetics, and the connections between the processing units and the sensors lead to complications if the wire paths are not well designed [11,12]. However, the use of sensors allows systems to achieve high performance, functionality, lower cost and greater accessibility compared to fiber-based solutions. Although these types of solutions are easier to integrate and address electrically, they suffer from limited performance and, more importantly, are more difficult to access (in terms of market and cost terms) and replace if damaged [11,12].

The type of sensor used and the method of measurement are key issues. Several investigations have used piezoresistive and piezoelectric effects, or both, as the basis for operation. Detection systems based on the piezoelectric effect use mechanical deformation to produce an electrical signal that varies proportionally with the amount of strain [13]. Typically, these types of systems are used in the design of systems wherein the objective is to detect and locate active forces rather than measure them quantitatively, as piezoelectric sensors are less accurate than piezoresistive ones. Well-known examples of this type of system are applied in the mapping of foot pressure in footwear, which can reveal gait patterns and weight distribution of patients undergoing rehabilitation to improve their movement recovery, and professional athletes, who use the system to improve training and performance [3,14].

By choosing to separate mechanical and sensory systems, the piezoelectric sensors are not implemented in the prosthetic hand, but rather in a multi-layer material that could cover the hand as a whole or be applied individually to its surface. This leads to long-term complications in experimental protocols, as the movement of the hand to grasp objects causes deformation of the piezoelectric sensors, generating false interaction signals. In this sense, the use of the piezoresistive effect has been exploited and studied as a means of generating touch by introducing piezoresistive sensors in specific areas of the sensory glove [10,13,14]. This type of system allowed for more adequate data collection and was a low-cost and high-functioning solution capable of quantifying and locating interactions between the surface of the prosthetic hand and objects. Piezoresistive sensing allows further integration of the sensing element into the robotic hand, for example, through conductive polymers [15] or composites [16].

This work proposes the design of a low-cost sensory glove system that complements the functioning of a 3D-printed mechanical hand prosthesis. The first objective is the production of the robotic hand model by 3D printing that is fast, low-cost and capable of acting by a mechanical movement control system. Then, we performed instrumentation of a glove capable of "feeling", locating and quantifying external forces. We believe this work to be of great interest not only scientifically but also socially, paving the way for the design and construction of hybrid systems that are coupled to the patient's body and communicate with it, just as the body communicates with the system. In addition, this work was motivated and inspired by the development of a personalized solution for a member of our academy who, for financial reasons, has not had access to this type of technology.

2. Three-Dimensional Printing of the Prosthesis

At the manufacturing level, the production method was critical to maximizing functionality and cost. Utilizing 3D printing allowed the choice of different types of material depending on the specific purpose of each part of the robotic hand. The chosen prosthetic

model was taken from an open-source research platform, which allowed the needs of each part to be quickly identified and the model to be divided into sections, with the hand and forearm being separate parts. All 3D prints were made on a *Prusa I3 MK3S+* printer with a building volume of 25 × 21 × 21 cm (XYZ) and a standard nozzle size of 0.4 mm. The printer itself is connected and programmed through its own software called *Prusa Slicer*, which allows the user to fully control every aspect of the production phase, allowing control in production speed, axis speed movement, layer weight, positioning on the feeding bed, percentage in support use, etc.

For the robotic hand, the raw material chosen had to be able to withstand considerable mechanical stress (tensile and flexural strength), since the fingers, the middle of the hand and the palm would be subjected to mechanical forces generated by servomotors during the instrumentation of the prosthesis. There were several materials that could have been used, such as polycarbonate (PC) and polyamide (PA) (nylon), but PLA was chosen as the raw material for the hand parts due to its cost effectiveness and long-term production characteristics. It provided the required tensile and flexural strength for each part, while allowing production time to be reduced. In contrast, the other polymers mentioned would provide greater tensile strength, but would increase production time and would be difficult to handle in the 3D printer, causing problems such as clogged nozzles, among others [17,18].

Each part was printed separately (Figure 1), allowing more accurate production customization and cost savings. Each part was monitored for size, geometric position on the print bed, infill percentage, layer weight, support percentage, ironing, surface quality, print speed and nozzle diameter. These parameters affect the production time, especially the geometric position, as it can change the amount of support material and can change the layer deposition during printing, affecting the strength of the part and the orientation of the layer.

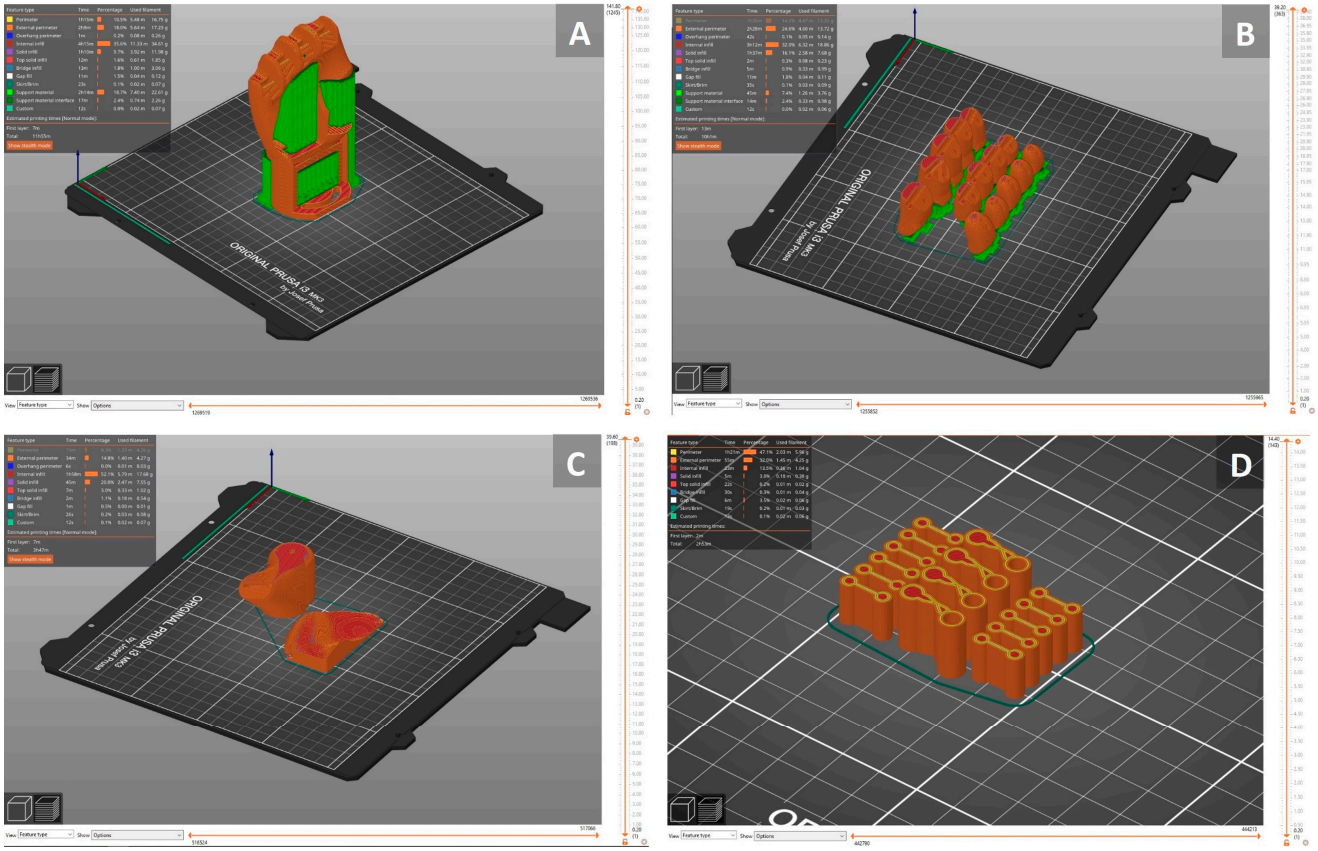

Figure 1. Representation of each of the parts of the prosthetic hand: (**A**) the core piece of the hand; (**B**) all the phalanges of each finger; (**C**) the attachments to the core of the hand: on the left, the attachment of the thumb, which allows it to move more freely; and on the right, the completion of the palm; (**D**) the attachments between the different phalanges, which allow the fingers to move.

Depending on the size of the part, the infill percentage can be changed, as parts with larger dimensions tend to reduce the infill percentage, compared to smaller parts. This parameter also has a significant effect on production time. Another aspect taken into account was the aesthetics of the robotic hand, i.e., the surface quality of the printed parts, which plays a fundamental role not only for the prosthesis user but also for the efficiency of the sensory system, since the surface of the palm and associated irregularities influence the magnitude of the touch felt by the sensors [18,19].

As mentioned above, each part was printed using specific polymeric 3D printing materials, which varied from part to part depending on the end use. Figure 1A–C shows the parts produced using PLA as the primary material. The only parts wherein PLA was not used are shown in Figure 1D. These specific parts were used for the attachments between the prosthetic fingers (Figure 1B), allowing them to move against each other, making the general movement of the prosthetic hand similar to the movement of a human hand. In this sense, the commercial polyurethane elastomer "FLEX" was chosen for this purpose because of its excellent flexibility and toughness, which allowed the parts to be moved very easily without damaging the material. However, due to the flexibility of its filament compared to PLA, this type of polymer presents some difficulties in terms of print management, so the temperature of the print bed and the printer as well the nozzle must be constant, without failures or inconsistencies during the printing process. The print bed temperature was 85 °C and the nozzle temperature was 250 °C. Variations in these temperatures result in the parts not sticking to the print bed and the nozzle feed channel clogging up, interrupting the flow of filament. The production of the forearm parts followed the same methodology as above, taking into account the same parameters, focusing on the final quality of the part, reducing the production time and, thus, the final cost. Table 1 shows a summary of the manufacturing conditions of the various parts, including percentage of material used in perimeter, internal infill and printing time.

Table 1. Manufacture conditions of the different 3D-printed parts of the prosthetic hand.

Part	Material	Internal Infill (%)	Perimeter (%)	External Perimeter (%)	Support (%)	Printing Time (minutes)
Arm parts:						
Forearm base	PETG	45.8	17.2	30.6	-	548
Lower part of the forearm		43.5	19.3	30.0	-	522
Forearm coverage		20.4	16.0	24.7	25.1	314
Hand	PLA	35.6	10.5	18.0	21.1	715
Palm cover		20.4	16.0	24.7	25.1	314
Thumb		20.4	16.0	24.7	25.1	314
Articulations parts between hand and fingers	FLEX	13.5	47.1	32.0	-	173
Articulations parts between phalanges						
Proximal phalanges	PLA	32	14.2	24.6	9.6	601
Medium phalanges						
Distal phalanges						

As the forearm is the only part of the robotic hand in direct contact with the end user, PETG polymer was chosen because it is biocompatible, ensuring greater compatibility with the end user. In addition, the material had to be able to be modified, if necessary, for instrumentation of the robotic hand without losing its structural integrity or being damaged in any way, and PETG offered the possibility of machining the part easily and without problems after printing. Its production settings, unlike those of FLEX, make it, like PLA, easier to use with few complications in the long-term production phase.

To aid decision making in the 3D printing process, the 3D rendering program evaluated the 3D models as changes were made, based on the production/printing data, through the various parameters mentioned above, thus helping to evaluate the best course of action. Figure 2 shows the final result of the 3D printing of the entire prosthetic limb, together with details of the inner part of the hand.

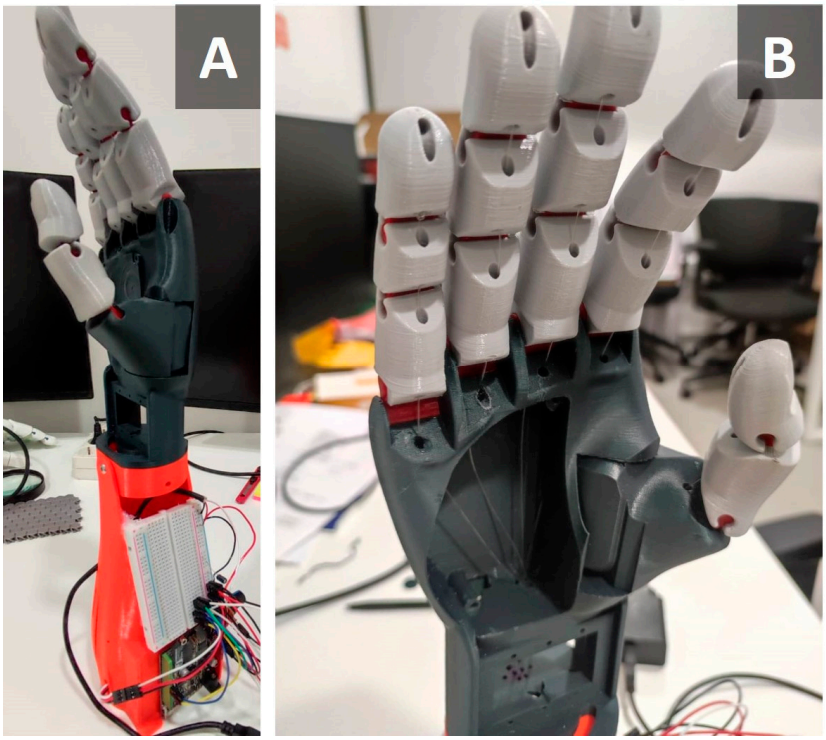

Figure 2. (**A**) Side view of the printed prosthetic limb; (**B**) view of the inside of the prosthetic hand.

3. Robotic Hand Instrumentation

3.1. Description of the Materials and Hardware

In the instrumentation of the prosthetic hand, two main factors were considered: cost reduction and the most functional system possible. In this sense, the choice between different hardware systems was fundamental to achieving both objectives, as was the design of the circuit and its assembly. For example, a simpler approach was taken by replacing the design and manufacture of a custom printed circuit board (PCB) with an *Arduino UNO*, a system that allows the same functionality as the PCB, with the advantage of being off-the-shelf and easily accessible.

To allow mechanical movement of the prosthetic hand, two *Zhiting* 270° 25 kg servomotors were placed on the main part of the forearm, each perpendicular to the corresponding wires attached to the prosthetic fingers (Figure 3). In this way, the wires are kept in a straight position from the fingers to the motors, allowing more direct control and faster response when the motor applies force to the wires, so that the prosthetic fingers work immediately and without delay.

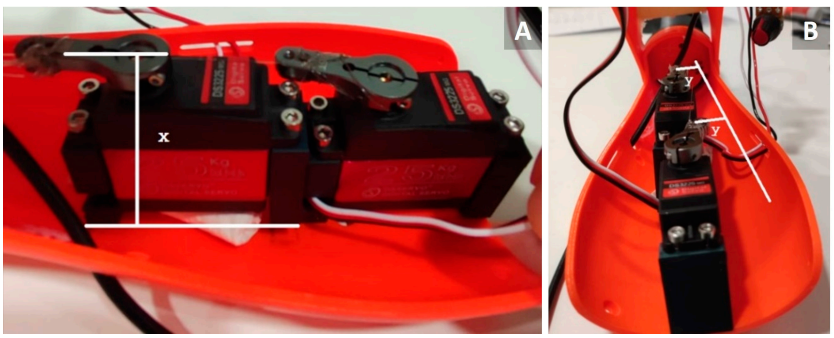

Figure 3. Representation of: (**A**) placement of the servomotors on the main part of the forearm, taking into account the height between the motor head and the main part (x); (**B**) alignment between the servomotors and the wires that control the finger movements (y).

In order to improve the functionality of the robotic hand and provide a greater range of motion for the thumb, the control of the movements of this finger was separated from the rest of the hand, with one servomotor for the function of the index, middle, ring and little fingers, and a second servomotor for the thumb only. Two potentiometers were used to control the servomotors, each controlling a specific servomotor. This allowed more precise, dynamic and real-time control of the force exerted by each of the servomotors on the prosthetic fingers, which in turn allowed greater accuracy in the subsequent measurement of the forces detected by the sensory system. The final result of the instrumentation assembly is shown in Figure 4.

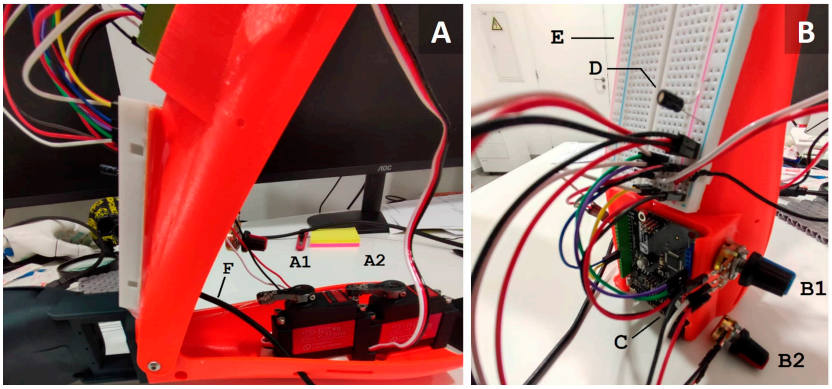

Figure 4. Illustration of an instrumented robotic hand: (**A**) servomotors (A1 and A2) and power cable (F); (**B**) potentiometers (B1 and B2), *Arduino UNO* (C), capacitor (D) and breadboard (E).

3.2. Software/Routine Code Description

The entire programming and control of the mechanical prosthetic system also followed a simplified approach, focusing on controlling the rotation of the servomotors and controlling the force applied to the wires that allow the prosthetic fingers to move. The rotation of the motors was controlled by potentiometers, each connected to a specific servomotor. In the following, servomotor M1, responsible for the movement of the index, middle, ring and little fingers, was connected to potentiometer A, and servomotor M2, responsible for the movement of the thumb, was connected to potentiometer B.

As the focus of this research is the implementation of a sensory system in the robotic hand, there was no need to extract specific results or values from the servomotors, only to control the movement of the prosthetic fingers as much as possible. To do this, it was necessary to implement a signal filter to refine the control of the motors when the potentiometers were activated, thus moving the servomotors. This filter was applied by connecting the analogue pin of the *Arduino UNO* to a data array. Each set of data was stored in its own array, one for each motor. When the potentiometer was activated, there were variations in the electrical resistance, and each variation corresponded to a certain amount of force produced by the servomotor. These variations were the results stored in the array. As these variations occurred, errors began to accumulate due to constant signal interference and delays in the exchange of information between the servomotor, the potentiometer and the *Arduino* system, leading to inaccurate control of the servomotor and, consequently, the prosthetic fingers. The filter continuously calculated the average between the previous signal stored in the array and the signal being read, thus reducing the overall signal errors by refining the servomotor control.

4. Robotic Hand Sensing

4.1. Description of the Materials/Hardware

Following the same methodology as the instrumentation, the sensory system was implemented with a focus on cost reduction while maintaining the performance of the system. It was also important that the sensory system was removable and independent of the limb instrumentation, so that the end user could decide whether to include it or

make the robotic hand even more economical. A breathable polyester-based glove with a polyurethane coating on the palm and fingertips was used as the basis for the sensory system. The proposed system consisted of sixteen piezoresistive sensors attached to the glove in certain key areas of interest (Figure 5), allowing more accurate detection of the prosthetic hand's interactions with objects and the measurement of forces and their locations.

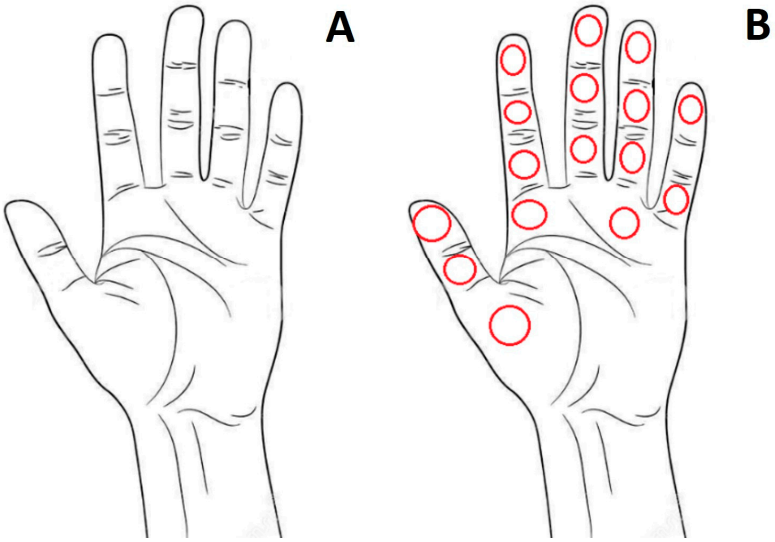

Figure 5. Representation of: (**A**) prosthetic hand; (**B**) locations where the sixteen piezoresistive sensors were placed.

The piezoresistive sensors used were force resistive sensors (*FRS*) from the 400 series, model *FRS402*, shown in Figure 6, a device based on a thick polytetrafluoroethylene (PTF) polymer film that exhibits a decrease in electrical resistance when a force is applied to its active surface. It has a circular detection area of 1.27 cm, an overall length of 6.0325 cm and a width of 1.905 cm. This type of sensor has a suitable sensitivity range (100 g to 10 kg) and measuring range (12.7 mm) [20]. Its morphology made it easy to install in the glove, as the strip fixed in the measurement area allowed a simplified connection between the sensor and the *Arduino*. The FSR402 sensor has been used in similar research to measure forces in a variety of applications [21,22]. According to [10], this type of sensor is suitable for detecting pressure differences on prosthetic surfaces.

Figure 6. Illustration of the FRS402 piezoresistive sensor used.

Due to the large number of sensors used in the assembly of the sensory glove, the processing unit had to provide a large number of simultaneous analogue read inputs. This led to the choice of the Arduino Mega2560, which has a total of sixteen analogue inputs.

The design of the glove's instrumentation again took a simplified approach, using the *Arduino Mega2560* (5 V) as the power supply controller, unlike the mechanical system instrumentation which was powered directly, reducing signal interference to the sensors. Following the manufacturer's assembly guidelines, each sensor was assembled using a current divider as shown in Figure 7.

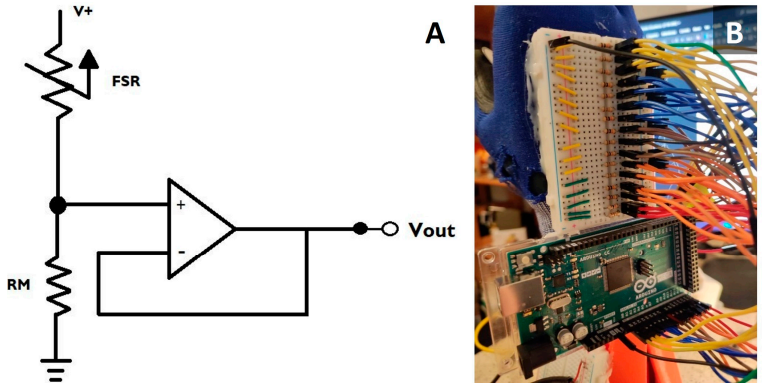

Figure 7. (**A**) The electric circuit used in each *FSR402* piezoresistive sensor; (**B**) final assembly of the circuit for the sensor glove.

4.2. Description of the Materials/Hardware

Due to the large number of sensors used, the programming of the system was carefully considered, as the *Arduino Mega2560* only had one analogue-to-digital converter (ADC), which allowed only one reading and one input each time the system was used. To overcome this limitation, a simple toggle function was implemented to make the sensors work one at a time by selecting the number that identifies each sensor and its specific position (Figure 8). In this way, the difference between simultaneous or individual functionality of the sensors did not have a major impact on the final results.

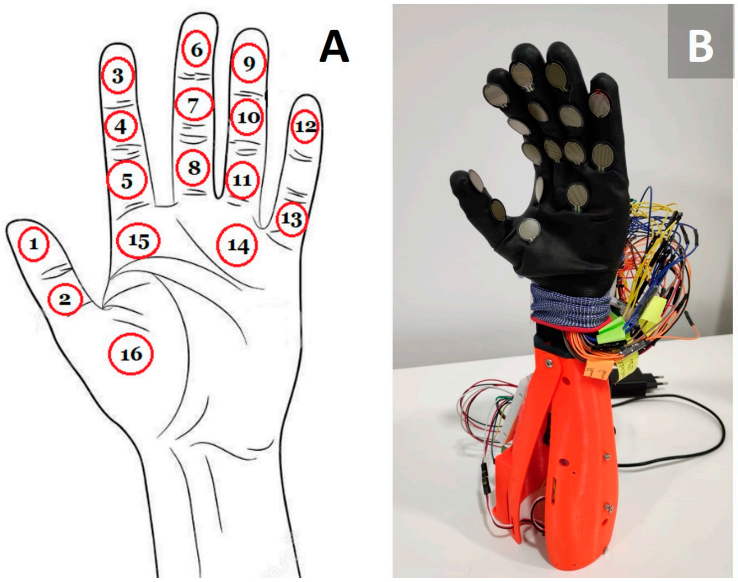

Figure 8. (**A**) Identification of each sensor by number (from 1 to 16), allowing measurement and identification of the specific area where interactions occurred; (**B**) the glove sensor system mounted.

5. Functionality Tests

The five tests described below were carried out to assess the functionality of the robotic hand. These tests were designed to validate not only the functionality of the mechanical system, but also that of the sensory system, in order to establish a correlation between the application of force, its measurement and location. The tests were divided according to daily activities as a basis for formulation:

- First Test: Grab a plastic cup;
- Second Test: Grab the same plastic cup with 150 mL of water;
- Third Test: Grab an empty plastic cup with larger dimensions;

- Fourth Test: Grab an egg;
- Fifth Test: Give a person a handshake.

The tests were carried out with objects of different weights, sizes and sensitivities. As this research is proposing the development of a sensory system, it also made sense to include a more human test that simulates human interaction, such as a simple handshake.

5.1. First Test—Grab a Plastic Cup

For this experiment, the protocol design was quite simple and effective, allowing the same steps to be carried out in all the other experiments. The steps were as follows:

1. Place the empty cup in the open prosthetic hand;
2. Move the thumb finger first;
3. Move the index, middle, ring and little fingers at the same time;
4. Before moving the fingers further, check that the cup is well positioned in the palm of the prosthetic hand;
5. Continue to move the fingers, increasing the force applied to the cup;
6. Lift the robotic hand with the cup;
7. If the cup falls, return to step 1;
8. If the cup is firm in the hand, take measurements and check the results.

The test is shown in Figure 9 and the results are shown in Figure 10 and Table 2.

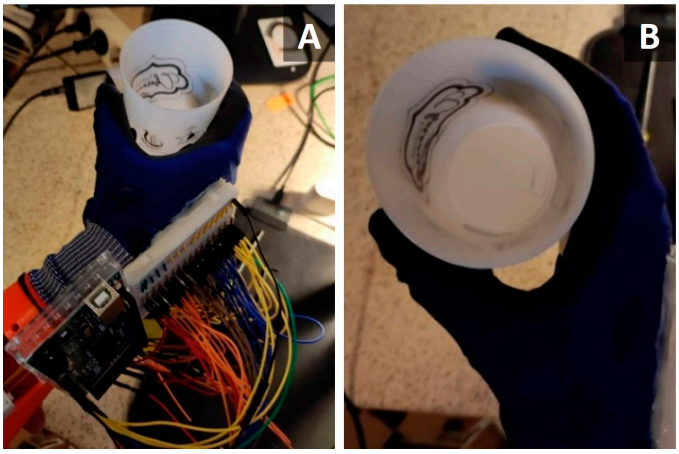

Figure 9. Illustration of the first experiment, grab an empty plastic cup. (**A**) general view; (**B**) top view.

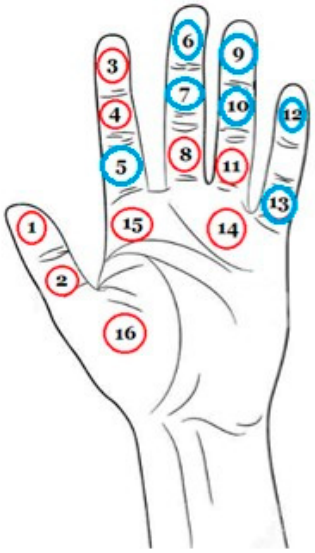

Figure 10. Representation of the activated sensors (blue circles) that detected interactions in the 1st test.

Table 2. Results obtained by the measurements taken from the 1st test.

Sensor	Analog Reading	Voltage (mv)	FSR Resistance (Ω)	Conductance (S)	Force (N)
A(1)	163	796	52,814	18	0
A(2)	0	0	0	0	NP *
A(3)	0	0	0	0	NP *
A(4)	0	0	0	0	NP *
A(5)	701	3431	4573	218	2
A(6)	918	4491	1133	882	10
A(7)	478	2336	11,404	87	1
A(8)	0	0	0	0	NP *
A(9)	558	2727	8335	119	1
A(10)	776	3792	3185	313	3
A(11)	0	0	0	0	NP *
A(12)	510	2492	10,064	99	1
A(13)	770	3763	3287	304	3
A(14)	0	0	0	0	NP *
A(15)	0	0	0	0	NP *
A(16)	0	0	0	0	NP *

* NP—No pressure.

Data analysis showed that there were more interactions in the middle, ring and little fingers. These interactions are explained by the nature of the movement of the prosthetic hand in relation to the plastic cup, causing these three fingers to support the cup. It is logical that the interactions with the plastic cup would be felt where the cup interacted most with the hand, as these fingers supported the cup to prevent it from falling. There were eight active sensors and a maximum force of 10 N was recorded on sensor A(6), at the tip of the middle finger. The average force recorded from the set of all interactions between the glove and the object was 2.63 N.

5.2. Second Test—Grab the Same Plastic Cup with 150 mL of Water

The second test used the same cup as the first but added 150 mL of water to increase the weight lifted by the hand. The protocol used was the same as in the first test, which made it possible to compare the results and observe differences in the interactions between objects of the same shape but different weights. The results are shown in Figure 11 and Table 3.

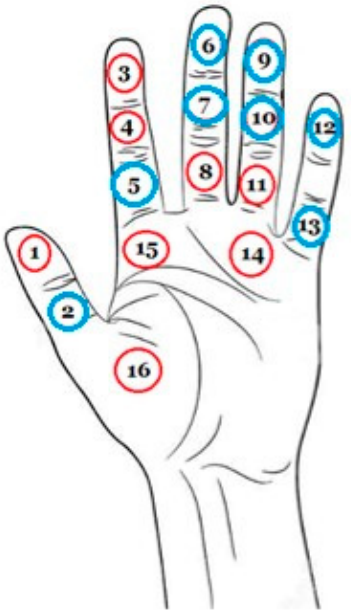

Figure 11. Representation of the activated sensors (blue circles) in the 2nd test.

The results of the second test are in line with expectations and confirm an increase in the number of activated sensors, mainly in the areas of the middle, ring, little and thumb fingers, due to a greater number of interactions between the cup and the robotic

hand caused by the increased weight of the cup. The value of the measured forces also increased compared to the results of the first test. The increased weight of the cup led to an increase in the total forces detected along the sensory system and in the active sensors, which recorded nine interactions. However, a greater distribution of forces was observed and the maximum value, also in sensor A(6), reached 6 N. The average force was 2.22 N, representing a decrease of ≈15% compared to the first test. This decrease can be explained by the increase in the number of active sensors registering very low interactions (≈0 N) which resulted in a greater distribution of the interactions felt along the sensory glove.

Table 3. Results obtained by the measurements taken from the 2nd test.

Sensor	Analog Reading	Voltage (mv)	FSR Resistance (Ω)	Conductance (S)	Force (N)
A(1)	194	948	42,742	23	0
A(2)	589	2878	7373	135	1
A(3)	0	0	0	0	NP *
A(4)	0	0	0	0	NP *
A(5)	793	3875	2903	344	4
A(6)	853	4169	1993	501	6
A(7)	724	3538	4132	242	3
A(8)	0	0	0	0	NP *
A(9)	159	777	54,350	18	0
A(10)	695	3396	4723	211	2
A(11)	0	0	0	0	NP *
A(12)	89	434	105,207	9	0
A(13)	813	3973	3584	386	4
A(14)	0	0	0	0	NP *
A(15)	0	0	0	0	NP *
A(16)	0	0	0	0	NP *

* NP—No pressure.

5.3. Third Test—Grab an Empty Plastic Cup with Larger Dimensions

As in the previous tests, the same protocol was followed, with the exception of the cup used, which had a larger diameter (Figure 12). The increase in cup size and the difference in surface morphology predicted an increase in the number of activated sensors and force values compared to the first test. The results are shown in Figure 13 and Table 4.

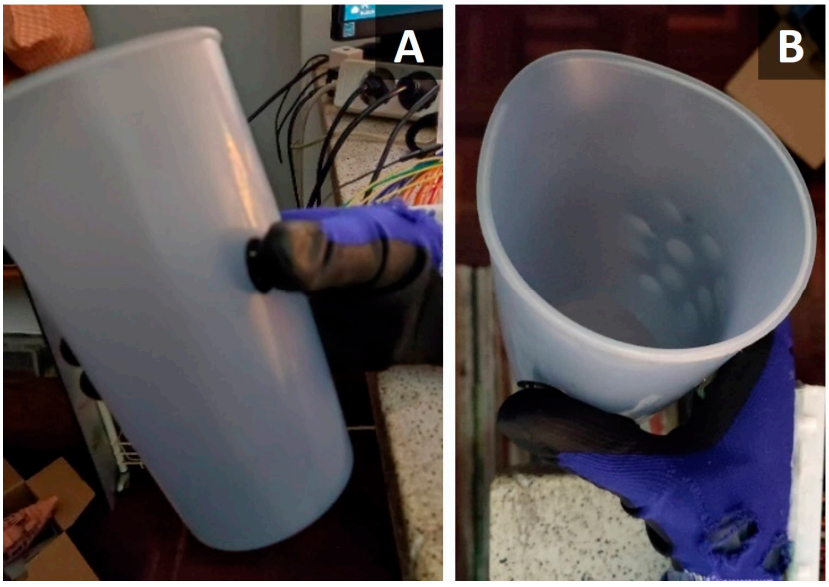

Figure 12. Third experiment with a larger plastic cup. (**A**) lateral view; (**B**) top view.

The results showed an increase in the number of active sensors compared to the first test, with eight sensors activated, mainly in the periphery and in the palm of the hand, specifically sensors A(2) and A(16). This was a consequence of the increase in the diameter of the cup, which led to an increase in the area of activity in the most central zone of the palm. As the cup was empty and the only weight felt on the surface of the hand was the

weight of the cup itself, the maximum force detected was relatively low, in the order of 6 N. The average force was 1.5 N, a reduction of around 43% compared to the first test, which can also be attributed to the greater number of active sensors that provide the force distribution.

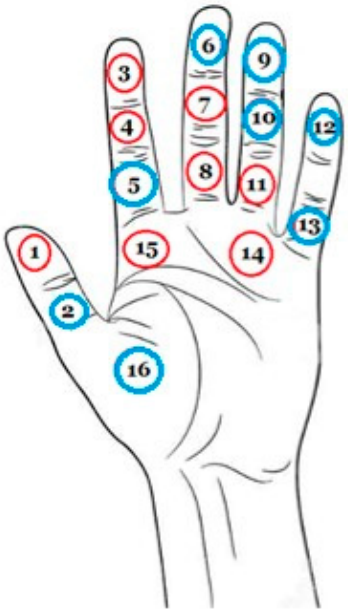

Figure 13. Representation of the activated sensors (blue circles) in the 3rd test.

Table 4. Results obtained by the measurements taken from the 3rd test.

Sensor	Analog Reading	Voltage (mv)	FSR Resistance (Ω)	Conductance (S)	Force (N)
A(1)	201	982	40,916	24	0
A(2)	769	3758	3304	302	3
A(3)	0	0	0	0	NP *
A(4)	0	0	0	0	NP *
A(5)	866	4232	1814	551	6
A(6)	698	3411	4658	214	2
A(7)	0	0	0	0	NP *
A(8)	0	0	0	0	NP *
A(9)	176	860	48,139	20	0
A(10)	505	2468	10,256	97	1
A(11)	0	0	0	0	0
A(12)	623	3044	6425	155	1
A(13)	704	3440	4534	220	2
A(14)	0	0	0	0	NP *
A(15)	0	0	0	0	NP *
A(16)	41	200	24,000	4	0

* NP—No pressure.

5.4. Fourth Test—Grab an Egg

The purpose of this test was to evaluate the sensitivity of the robotic hand. In order to grasp the egg without damaging it (Figure 14), the mechanical and sensory system had to be well calibrated to precisely control the force exerted by the servomotor on the cables that move the prosthetic fingers and detect small interactions and quantify small forces. For this test, it was assumed that the number of active sensors would be smaller than in previous tests and that the forces detected would be smaller. The results are shown in Figure 15 and Table 5.

The results show a reduction in both the number of active sensors in the hand–object interactions and the force value. The areas of interaction were small and very specific, with greater activity in the middle, ring and thumb fingers. In terms of force levels, the thumb A(2) and the middle fingertip A(6) dominated with 3 N and 4 N, respectively. The other interactions were not significant enough to generate measurable force values, but the low voltage and high resistance values indicate the detection of small interactions between the

sensor and the object. This test also proved that the calibration of the servomotors allows fine and delicate movements.

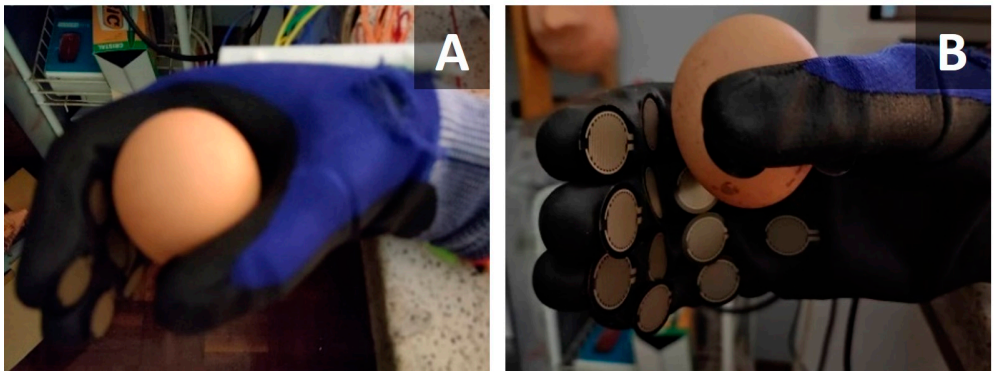

Figure 14. Illustration of the 4th test, grabbing an egg.

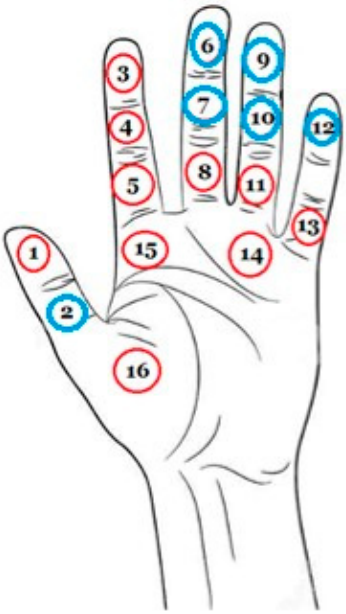

Figure 15. Representation of the activated sensors (blue circles) in the 4th test.

Table 5. Results obtained by the measurements taken from the 4th test.

Sensor	Analog Reading	Voltage (mv)	FSR Resistance (Ω)	Conductance (S)	Force (N)
A(1)	196	957	42,246	23	0
A(2)	757	3699	3517	284	3
A(3)	0	0	0	0	NP *
A(4)	0	0	0	0	NP *
A(5)	0	0	0	0	NP *
A(6)	799	3905	2804	356	4
A(7)	175	855	48,479	20	0
A(8)	0	0	0	0	NP *
A(9)	147	718	59,637	16	0
A(10)	168	821	50,901	19	0
A(11)	0	0	0	0	NP *
A(12)	113	552	80,579	12	0
A(13)	0	0	0	0	NP *
A(14)	0	0	0	0	NP *
A(15)	0	0	0	0	NP *
A(16)	0	0	0	0	NP *

* NP—No pressure.

5.5. Fifth Test—Give a Person a Handshake

As the main focus of this research is the development of touch detection, it made sense to develop a test that simulated one of the simplest human interactions, a handshake (Figure 16). For this test, the expected result was a greater number of active sensors (Figure 17), as the human hand would be in contact with a superior surface area when interacting with the sensory glove. Depending on the force exerted by the human hand on the sensory glove and vice versa, the results of the forces detected varied. Figure 17 and Table 6 show representative results.

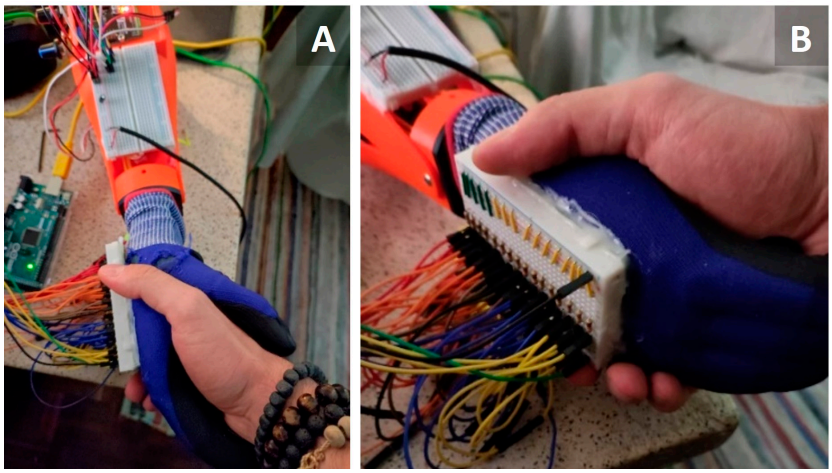

Figure 16. Illustration of the 5th test, giving a person a handshake. (**A**) top view; (**B**) lateral view.

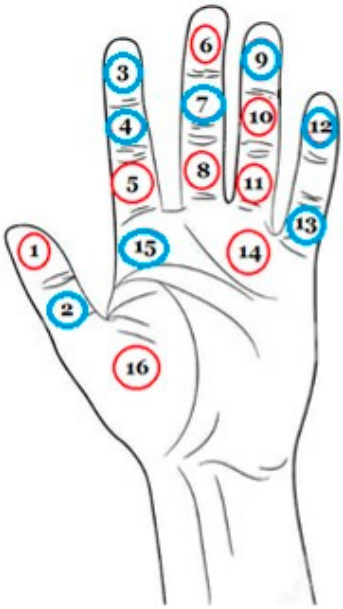

Figure 17. Representation of the activated sensors (blue circles) in the 5th test.

In this test, it was essential to control the force applied by the servomotor so that it was not so high as to harm the subject. By setting the forces produced by the servomotor to a minimum value, the results showed, as expected, that the number of active sensors was greater than in any other test, showing activity in more generalized areas (central and peripheral). As the forces applied to the human hand were small, the forces measured were also small, in the order of 4 N. As in the previous test, the interactions detected were of low intensity and, therefore, could not result in significant force values. However, the low stress values and, consequently, the high resistance values proved that there were small interactions between the surface of the prosthetic hand and the object.

Table 6. Results obtained by the measurements taken from the 5th test.

Sensor	Analog Reading	Voltage (mv)	FSR Resistance (Ω)	Conductance (S)	Force (N)
A(1)	200	977	41,177	24	0
A(2)	787	3846	3000	333	4
A(3)	488	2385	10,964	91	1
A(4)	684	3362	4872	205	2
A(5)	0	0	0	0	NP *
A(6)	0	0	0	0	NP *
A(7)	3	14	3,561,428	0	0
A(8)	0	0	0	0	NP *
A(9)	157	767	55,189	18	0
A(10)	0	0	0	0	NP *
A(11)	0	0	0	0	NP *
A(12)	82	400	115,000	8	0
A(13)	96	469	96,609	10	0
A(14)	0	0	0	0	NP *
A(15)	7	34	1,460,588	0	0
A(16)	0	0	0	0	0

* NP—No pressure.

6. Conclusions

The attribution of somatosensory properties (touch sensation) to an upper arm prosthesis, making both the fabrication of the robotic hand and its instrumentation (mechanical and sensory) as affordable as possible, was successfully achieved.

Considering the model of the prosthesis used and the patient-centered methodology, it was possible to achieve the highest quality and functionality of the robotic hand at the lowest possible cost. In addition, by mimicking the design of the human arm, it was possible to provide a system with functionality close to that of the human hand, giving the thumb a greater range of movement. In terms of aesthetics, the prosthetic fingers and palm closely mimicked the surface characteristics of the human hand, with uneven and rounded surfaces. This was made possible by the use of 3D printing, which allowed the customization of each parameter of the manufacturing phase (filling, ironing, layer weight, etc.), producing a high-quality, low-cost prototype that could be easily instrumented and modified as needed and for which the sensory system could be easily installed and removed.

The instrumentation of the mechanical system followed a simplistic approach, using simple off-the-shelf components that could be easily replaced if damaged without significantly increasing the cost. The programming of the overall mechanical system focused on refining the motor control to allow more precise hand movements and, thus, control of the force exerted by the prosthetic hand on the objects with which it interacts.

By defining the piezoresistive sensor as the main sensing element, the assembly of the sensing glove and its application to the prosthetic hand were straightforward. As the *Arduino* has only one ADC converter, the programming followed a select-sensor approach, making it possible to locate and measure the interactions between the sensing glove and the specific object at a given moment or continuously, millisecond by millisecond. As with the mechanical system, in the event of malfunction or damage, any part of the sensing glove can be easily replaced at a low cost to the user.

The overall test results provided the expected results and predictions, allowing the design and construction of an advanced and cost-effective prosthetic system capable of detecting touch and measuring force which can be designed and customized for each user without increasing the overall cost and allows easy replacement of any part in the event of damage or excessive use. The promising results of this research make this approach an effective tool for the production of customizable prosthetic systems with the possibility of interaction in both directions: patient–prosthesis and prosthesis–patient.

Author Contributions: Conceptualization, G.F., J.N.-P. and A.P.S.; methodology, G.F., J.N.-P. and A.P.S.; software, G.F.; validation, G.F., J.N.-P. and A.P.S.; formal analysis, J.N.-P. and A.P.S.; investigation, G.F.; writing—original draft preparation, G.F. and J.N.-P.; writing—review and editing, J.N.-P. and A.P.S.; project administration, A.P.S. and J.N.-P.; funding acquisition, A.P.S. All authors have read and agreed to the published version of the manuscript.

Funding: This research was funded by the Portuguese Foundation for Science and Technology, I.P. (FCT, I.P.) FCT/MCTES through national funds (PIDDAC), under the R&D Unit C-MAST/Centre for Mechanical and Aerospace Science and Technologies (Project UIDB/00151/2020). João Nunes-Pereira would also like to thank FCT, I.P., for the contract under the Stimulus of Scientific Employment, Individual Support: 2022.05613.CEECIND.

Institutional Review Board Statement: Not applicable.

Informed Consent Statement: Not applicable.

Acknowledgments: The authors are grateful for the support of the Portuguese Foundation for Science and Technology, I.P. (FCT, I.P.) FCT/MCTES through national funds (PIDDAC), under the R&D Unit C-MAST/Centre for Mechanical and Aerospace Science and Technologies (Project UIDB/00151/2020). João Nunes-Pereira would also like to thank FCT, I.P., for the contract under the Stimulus of Scientific Employment, Individual Support: 2022.05613.CEECIND.

Conflicts of Interest: The authors declare no conflict of interest.

References

1. Dunn, J.; Runge, R.; Snyder, M. Wearables and the medical revolution. *Pers. Med.* **2018**, *15*, 429–448. [CrossRef]
2. Wearable Medical Devices: Technologies and Global Markets (HLC192C). 2022. Available online: https://www.bccresearch.com/market-research/healthcare/wearable-medical-devices.html (accessed on 2 November 2022).
3. Khoshmanesh, F.; Thurgood, P.; Pirogova, E.; Nahavandi, S.; Baratchi, S. Wearable sensors: At the frontier of personalised health monitoring, smart prosthetics and assistive technologies. *Biosens. Bioelectron.* **2021**, *176*, 112946. [CrossRef] [PubMed]
4. Colazo, J.M.; Koshy, K. A commentary on: "3D printing for developing patient specific cosmetic prosthetics at the point of care" [Int. J. Surg. (2020) Epub ahead of Print]. *Int. J. Surg.* **2020**, *82*, 121–122. [CrossRef] [PubMed]
5. Su, A.; Al'Aref, S.J. History of 3D Printing. In *3D Printing Applications in Cardiovascular Medicine*; Al'Aref, S.J., Mosadegh, B., Dunham, S., Min, J.K., Eds.; Elsevier: Amsterdam, The Netherlands; Academic Press: London, UK, 2018; pp. 1–10. [CrossRef]
6. Ventola, C.L. Medical Applications for 3D Printing: Current and Projected Uses. *PT* **2014**, *39*, 704–711.
7. Park, S.J.; Lee, J.; Choi, J.W.; Yang, J.H.; Lee, J.H.; Lee, J.; Son, Y.; Ha, C.W.; Lee, N.-K.; Kim, S.H.; et al. Additive manufacturing of the core template for the fabrication of an artificial blood vessel: The relationship between the extruded deposition diameter and the filament/nozzle transition ratio. *Mater. Sci. Eng. C* **2021**, *118*, 111406. [CrossRef]
8. Prusa, J. Technical Data Sheet—Prusament PLA, Prusa Polymers. 2022. Available online: https://prusament.com/media/2022/10/PLA_Prusament_TDS_2021_10_EN.pdf (accessed on 20 October 2022).
9. Prusa, J. Technical Data Sheet—Prusament PETG, Prusa Polymers. 2018. Available online: https://prusament.com/media/2018/09/Prusament_techsheet_PETG-1-1.pdf (accessed on 20 October 2022).
10. Polishchuk, A.; Navaraj, W.T.; Heidari, H.; Dahiya, R. Multisensory Smart Glove for Tactile Feedback in Prosthetic Hand. *Procedia Eng.* **2016**, *168*, 1605–1608. [CrossRef]
11. Leber, A.; Page, A.G.; Yan, D.; Qu, Y.; Shadman, S.; Reis, P.; Sorin, F. Compressible and Electrically Conducting Fibers for Large-Area Sensing of Pressures. *Adv. Funct. Mater.* **2020**, *30*, 1904274. [CrossRef]
12. Atalay, O.; Atalay, A.; Gafford, J.; Walsh, C. A Highly Sensitive Capacitive-Based Soft Pressure Sensor Based on a Conductive Fabric and a Microporous Dielectric Layer. *Adv. Mater. Technol.* **2018**, *3*, 1700237. [CrossRef]
13. Poplavko, Y.; Yakymenko, Y. Piezoelectricity. In *Functional Dielectrics for Electronics*; Poplavko, Y., Yakymenko, Y., Eds.; Woodhead Publishing: Sawston, UK, 2020; pp. 161–216. [CrossRef]
14. Navaraj, W.T.; Nassar, H.; Dahiya, R. Prosthetic Hand with Biomimetic Tactile Sensing and Force Feedback. In Proceedings of the 2019 IEEE International Symposium on Circuits and Systems (ISCAS), Sapporo, Japan, 26–29 May 2019. [CrossRef]
15. Pereira, J.N.; Vieira, P.; Ferreira, A.; Paleo, A.J.; Rocha, J.G.; Lanceros-Méndez, S. Piezoresistive effect in spin-coated polyaniline thin films. *J. Polym. Res.* **2012**, *19*, 9815. [CrossRef]
16. Fiorillo, A.S.; Critello, C.D.; Pullano, S.A. Theory, technology and applications of piezoresistive sensors: A review. *Sens. Actuators A Phys.* **2018**, *281*, 156–175. [CrossRef]
17. Valvez, S.; Silva, A.P.; Reis, P.N.B. Compressive Behaviour of 3D-Printed PETG Composites. *Aerospace* **2022**, *9*, 124. [CrossRef]
18. Valvez, S.; Silva, A.P.; Reis, P.N.B. Optimization of Printing Parameters to Maximize the Mechanical Properties of 3D-Printed PETG-Based Parts. *Polymers* **2022**, *14*, 2564. [CrossRef]
19. Monteiro, J.; Carrilho, J.; da Silva, M.G.; Miranda, A.; Silva, A. 3D Printed Pressure Anemometers. *3D Print. Addit. Manuf.* **2017**, *4*, 172–181. [CrossRef]

20. Interlink Electronics. FSR—Force Sensing Resistor Integrated Guide and Evaluation Parts Catalog, Interlink Electronics. Available online: https://www.sparkfun.com/datasheets/Sensors/Pressure/fsrguide.pdf (accessed on 5 October 2022).
21. Wibowo, D.B.; Suprihanto, A.; Caesarendra, W.; Khoeron, S.; Glowacz, A.; Irfan, M. A Simple Foot Plantar Pressure Measurement Platform System Using Force-Sensing Resistors. *Appl. Syst. Innov.* **2020**, *3*, 33. [CrossRef]
22. Tasakorn, M.; Charoenmee, A.; Jamsai, M.; Klongklaew, U.; Pherawan, J.; Phuphanin, A.; Boomeewised, K.; Prajudtasri, S.; Thongmee, S.; Jaratthanaworapat, A.; et al. A Low-Cost Force and Vibration Measurement Using FSR-402 and SW-420 Sensors for Sports Shoe Inspection. In Proceedings of the 2022 International Electrical Engineering Congress (iEECON), Khon Kaen, Thailand, 9–11 March 2022. [CrossRef]